Tracing Lithosphere Evolution through the analysis of Heterogeneous G9/G10 Garnets in Peridotite Xenoliths

Burgess, S.R. [1,2] and Harte, B. [1]

1. Department of Geology and Geophysics, University of Edinburgh, Kings Buildings, Edinburgh EH9 3JW, U.K.
2. Oxford Instruments Microanalysis Group, Halifax Road, High Wycombe, Buckinghamshire, HP12 3SE, U.K.

Introduction

Understanding the nature and evolution of variations in mantle lithosphere composition is a long term objective of mantle studies, and metasomatism has been attributed an important role in the geochemical evolution (e.g. Harte and Hawkesworth, 1989; McKenzie, 1989). Detailed studies of garnets in many peridotite xenoliths from Jagersfontein have shown them to be heterogeneous in chemical composition and linking these variations to the depths and temperatures of origin of the xenoliths has yielded important new evidence for the evolution of the sub-cratonic mantle through space and time (Burgess, 1997).

The studies have been carried out by first combining petrographic observations with detailed electron microprobe (EMP) analysis, including X-ray mapping using wavelength dispersive techniques of chemically zoned (or heterogenous) garnets, and then carrying out trace element analysis using high spatial resolution ion microprobe (IMP or SIMS) techniques. Both EMP and IMP analyses were done at Edinburgh University on Cameca Camebax and Cameca ims-4f instruments respectively, using standard techniques. Estimates of pressure and temperature for the xenoliths were determined following the recommendations of Brey and Kohler (1990). The mineral melt partition coefficients used for trace elements follow the suggestions of Harte et al. (1996).

Major-minor element compositions and the CaO-Cr_2O_3 diagram for Garnets

The types of compositional variations seen may be summarised on the CaO-Cr_2O_3 diagram, which is widely used for distinguishing lherzolitic (G9) from harzburgitic (G10) peridotite garnets and G10 (high Cr/low Ca) garnets associated with diamonds. On this diagram (see Fig. 1a) chemically homogeneous Jagersfontein garnets plot in reasonably distinct fields according with the division of the peridotite suite by Winterburn et al. (1990) into: (i) a coarse low-temperature lherzolitic suite; (ii) a coarse medium-temperature harzburgitic suite; and (iii) a deformed high-temperature suite (both lherzolites and harzburgites). The garnets from deformed high-temperature peridotites define the lherzolite trend line (Fig. 1), and are broadly distributed along this trend with Cr and Ca decreasing according to depth, so the deepest samples plot near the base of the lherzolite trend.

Representative peridotite-suite garnets showing core-rim zonation (or other chemical compositional heterogeneity) are also shown on Fig. 1a. As well as Ca and Cr, the variation in these heterogeneous garnets commonly involves Ti, Cr and Mg (sometimes Fe and Na), and a number of major types (Ia, Ib, II, IIIa and IIIb) of compositional variation may be distinguished as shown in Fig. 1b. By far the commonest core to rim variation seen involves decreasing Cr and Ca (Type I) in high-temperature lherzolitic (G9) garnets and moves them down the lherzolite trend. However some of the high-temperature and the deeper lherzolitic garnets move up the lherzolite trend (Type II, Fig. 1b). In addition harzburgitic (G10) garnets show core to rim variation taking them towards the lherzolite trend (Type III variation, Fig. 1b).

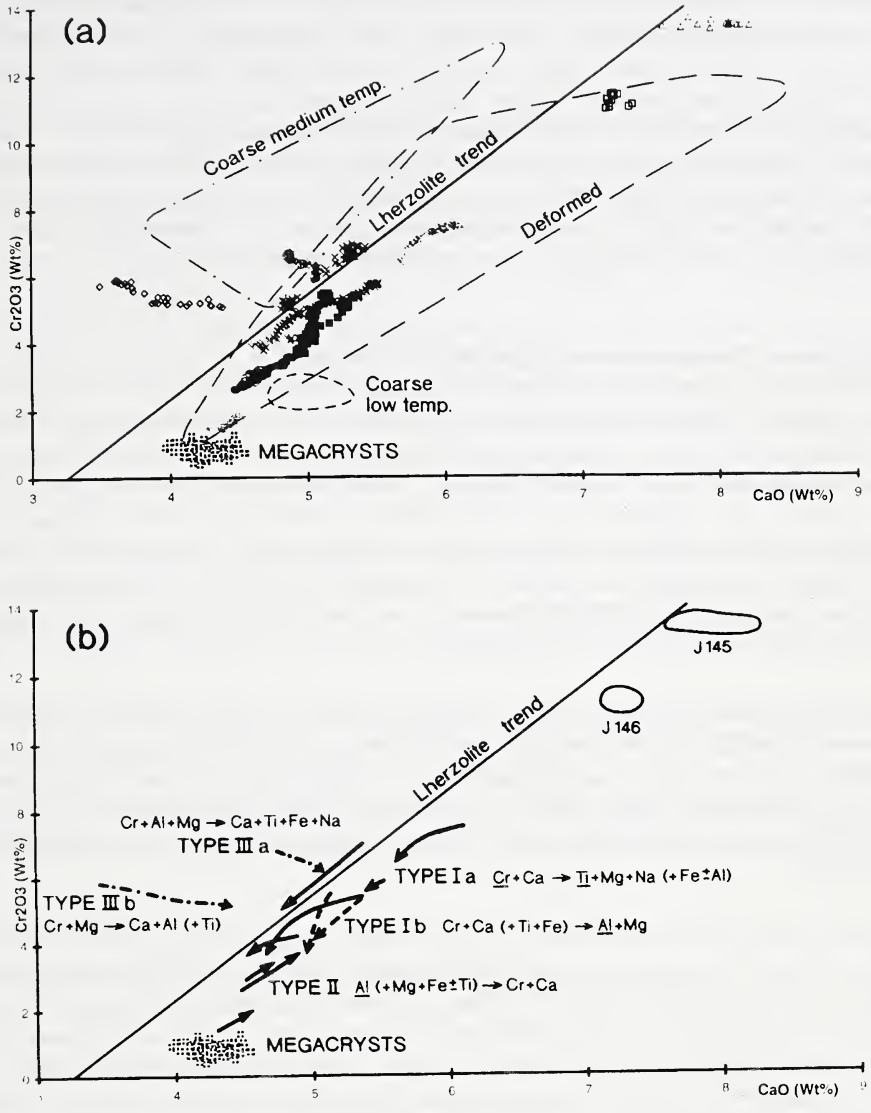

Fig. 1 Garnets of the Jagersfontein peridotite suite plotted in the CaO-Cr_2O_3 diagram.
(**a**) The dashed lines outline the main composition fields found for homogeneous garnets in:
(i) coarse low-temperature lherzoliths; (ii) coarse medium-temperature harzburgites; and (iii) deformed high-temperature lherzolites and harzburgites. The lherzolite trend line is defined by the high-temperature peridotites, which show greater depths of origin with decreasing Cr_2O_3 and CaO. For heterogenous garnets groups of identical symbols show individual composition points in representative garnets; with: crosses representing Type Ia, squares TypeIb, circles Type II, diamonds Type III. Compositions of megacrystic garnets from Jagersfontein are shown by square with cross symbols.
(**b**) Arrowed lines pick out the core-to-rim trends in composition of heterogeneous garnets plotted in upper diagram (a) and indicate major compositional variations. Megacrysts as in (a).

Burgess (1997) showed that the major-minor element compositional variations could be interpreted as due to metasomatic interaction with melts whose original compositions were similar to those of the magmas from which Cr-poor garnet megacrysts crystallised. As the melt infiltrated and percolated through the peridotites, its major element compositions were largely buffered by the peridotites, but less compatible elements remained unbuffered, and therefore minor elements such as Ti increased progressively as the melt moved upwards. Burgess (1997) therefore suggested that melt infiltration through the deformed mantle, and into the coarse cratonic root zone (represented by the G10-bearing harzburgitic medium-temperature xenoliths), caused the removal of G10 garnets and modification of harzburgites to lherzolites in the root zone over time.

Rare Earth Element Composition of Jagersfontein Garnets

The rare earth element composition of garnets is closely related to their depth and position on the CaO-Cr_2O_3 diagram. Coarse low-temperature G9-garnets from unmetasomatised samples have HREE-enriched garnet patterns with the overall lowest abundances of REE. Coarse medium-temperature G10-garnets show 'humped' patterns, widely thought to be characteristic of coarse xenolith garnets, with a maximum on the chondrite-normalised REE abundance diagram somewhere between Ce and Dy according to sample. Deformed high-temperature G9 garnets show dominantly HREE-enriched plateau patterns, with LREE-MREE lower in abundance than G10 garnets, but with higher levels of HREE. However, those with relatively high Ca-Cr exhibit minor maxima in the MREE, particularly in grain cores.

Core-to-rim compositional changes within a garnet are dominated by increases in HREE, with minor decreases in LREE. Therefore in the 'humped' patterns shown by G10 garnets, the maxima on the chondrite-normalised abundance diagram move toward the HREE as one moves from core to rim of the garnet. Relatively shallow, high Ca-Cr deformed G9 garnets change from 'humped' REE patterns to HREE-enriched plateau patterns. Deeper G9 garnets simply show increasing levels of the HREE plateau.

There is a clear compositional progression in garnet compositions in terms of REE which is coupled to Ca-Cr. As the Ca-Cr increases in deformed G9 garnets, the levels of LREE increase and levels of HREE decrease, whilst core-to-rim variations increase from indistinct changes in the deepest samples to marked changes in garnet-REE pattern shape in the shallower deformed peridotite samples. The coarse G10 garnets, derived from mantle overlying the deformed peridotite section, but representing the lower part of the coarse-xenolith mantle, provide an extension of this trend by showing further increases in LREE, decreases in HREE, and yet larger core-to-rim REE variations.

The Composition and Evolution of Melts in Equilibrium with Garnet

The expected trace element compositions of melts in equilibrium with garnet core and rim compositions have been calculated using partition coefficients. REE patterns of **melts in equilibrium with the rims of garnets** showing a range of CaO-Cr_2O_3 compositions are shown in Fig. 2a. All melt compositions are characterised by LREE-enrichment. In addition for deformed peridotite G9 garnets, as the garnet CaO-Cr_2O_3 composition increases and therefore depth of origin decreases, the LREE abundance and LREE/HREE ratio steadily increase (DP garnets in Fig. 2a). The composition of melt in equilibrium with a coarse G10 garnet (1728 G10 in Fig. 2a) represents a continuation of this trend to still higher LREE/HREE ratios. Also shown in Fig.2a is the composition of melt in equilibrium with a typical Cr-poor garnet megacryst (J75 MEG) from

Jagersfontein. Its composition, with the lowest LREE and highest HREE, is consistent with it representing the source composition of a melt which percolated upwards and evolved to progressively higher LREE/HREE as it went.

Similar plots of REE compositions of **melts in equilibrium with the core compositions** of large grains (representing earlier garnet compositions unlikely to have been modified by diffusion) show the same pattern of increasing LREE/HREE ratio as CaO-Cr_2O_3 compositions increase and therefore depth decreases. However, melts in equilibrium with cores have higher LREE/HREE ratios than those in equilibrium with corresponding rims, suggesting more 'evolved' compositions.

Theoretical modelling (Burgess 1997) of the evolution of an initial 'megacryst' melt composition (like J75 MEG in Fig. 2a) as a consequence of Rayleigh fractionation of olivine, pyroxene, and garnet is shown in Fig. 2b. The resultant calculated melt compositions (represented by melt proportions 1 to 0.1 in Fig. 2b) show REE compositions similar to those of melts in equilibrium with the rims of deformed G9 (DP) and coarse G10 garnets (Fig. 2a). These results indicate the importance of crystal fractionation in creating appropriate metasomatic melt compositions from an initial 'megacryst' melt as it percolates through and reacts with the sub-cratonic peridotites to produce the zoned garnets. Other processes, such as the reaction and exchange seen in a chromatographic column (Navon and Stolper 1987), may be important, but without crystal fractionation they cannot easily produce the increasing LREE/HREE signatures with decreasing depth from a 'depleted' archaean sub-cratonic lithosphere.

Clearly, segments of the mantle lithosphere may have been affected by such percolation-reaction-fractionation processes more than once, and, as well generating the rim compositons of the garnets under discussion, they could have played a role in creating the earlier core garnet compositions in the peridotites. It is notable that the melt fractionation process modelled in Fig. 2b is capable of generating melts from which garnets with markedly 'humped' REE patterns may crystallise.

Conclusions

Core-to-rim compositional variations in peridotitic garnets show systematic variations related to the initial core composition of the garnet and the depth of origin of the peridotites. Major-minor element compositional changes are consistent with metasomatic interaction with melts related to megacryst magma compositions, which cause changes in garnet composition along the G9 lherzolite trend and from G10 towards the G9 lherzolite trend. The REE compositions of the garnet rims are characterised by increasing LREE/HREE ratios, and may be modelled as those in equilibrium with a 'megacryst melt' undergoing crystal fractionation whilst percolating through and reacting with peridotites. Thus the metasomatic modification of the peridotites involves both reactional exchange and crystal fractionation, similar to the model of *percolative crystal fractionation* argued for on other grounds by Harte et al. (1993).

The correlation of major-minor-trace element compositions with depth-temperature relations and the CaO-Cr_2O_3 plot for garnets may be used to explain the evolution and distribution of G9/G10 garnets in the sub-cratonic lithsophere. In particular, the loss of G10 signatures in harzburgites by this process may be evidence for the modification of the cratonic root zone to lherzolitic compositions over time, and thus has implications for diamond distribution and productivity.

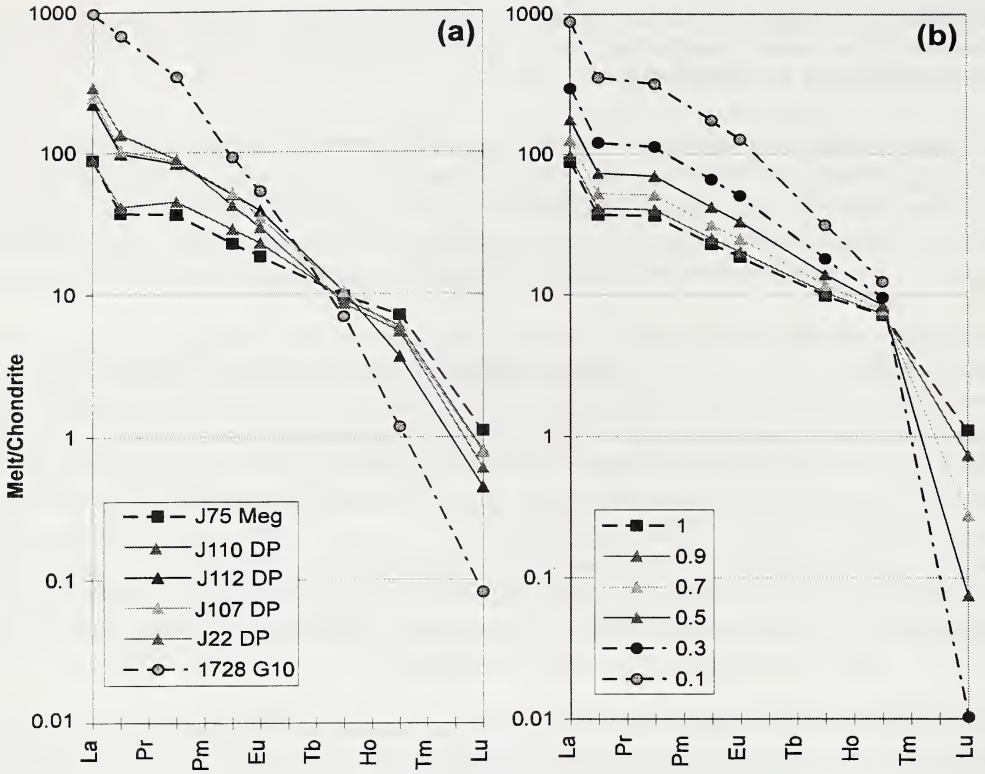

Fig.2. (**a**) REE compositions of melts calculated using partition coefficients (Harte et al., 1996) to be in equilibrium with garnet rim compositons ('J75 Meg' is a typical megacryst, the 'DP' are deformed high-temperature peridotites, and '1728 G10' is from a coarse medium-temperature harzburgite). (**b**) Theoretical melt compositons calculated on the basis of fractional crystallisation of 50% olivine, 25% garnet, and 25% clinopyroxene from an initial melt in equilibrium with the composition of the J75 megacryst. 0.9 to 0.1 labels indicate the proportion of melt remaining.

References

Brey, G.P., and Kohler, T., 1990, Geothermometry in four-phase lherzolites II: new thermometers, and a practical assessment of existing thermometers. J. Petrology, 31, p. 1353-1378.

Burgess, S. R., 1997, The evolution of the sub-cratonic mantle seen in mantle xenoliths: Unpub. PhD Thesis, University of Edinburgh.

Harte, B., Fitzsimons, I.C.W., Kinny, P.D., 1996, Clinopyroxene-garnet trace element partition coefficients for mantle peridotite and melt assemblages: V.M. Goldschmidt Conf. Abstr., 1, p. 235.

Harte, B., and Hawkesworth, C.J., 1989, Mantle domains and mantle xenoliths. Geol. Soc. Aust. Spec. Publ. No. 14, p. 649-686.

Harte B., Hunter R.H., and Kinny, P.D., 1993, Melt geometry, movement and crystallisation, in relation to mantle dykes, veins and metasomatism. Phil. Trans. Roy. Soc. Lond., A342, p.1-21.

McKenzie, D., 1989, Some remarks on the movement of small melt fractions in the mantle. Earth Plan. Sci. Letts., 95, p. 53-72.

Navon, O., and Stolper, E., 1987, Geochemical consequences of melt percolation: the upper mantle as a chromatographic column: Jour. Geol., 95, 285-307.

Winterburn, P.A., Harte, B., and Gurney, J.J., 1990, Peridotite xenoliths from the Jagersfontein kimberlite pipe: I. Geochim. Cosmochim. Acta, 54, 329-341.